PROCEEDINGS OF SPIE

SPIEDigitalLibrary.org/conference-proceedings-of-spie

Electro-optic polymer devices for optical interconnects

Richard S. Lytel
Edward S. Binkley
Dexter G. Girton
John T. Kenney
George F. Lipscomb
Anthony J. Ticknor
Timothy E. Van Eck

SPIE.

Electro-optic Polymer Devices for Optical Interconnects

R. Lytel, E.S. Binkley, D.G. Girton, J.T. Kenney, G.F. Lipscomb, A.J. Ticknor, and T. E. Van Eck

Lockheed Research and Development Division
Department 9701, Building 201
3251 Hanover St., Palo Alto, CA 94304

ABSTRACT

Electro-optic polymers exhibit many useful properties for distribution and routing of light on optical multilayer boards and modules. With the development of more robust materials, it should soon be possible to use these materials to provide high-density interconnects at significant power savings, and with reduced noise, at frequencies above 100 MHz. We review the research toward creating new materials and devices for applications to packaging technology.

1. INTRODUCTION

Organic and polymeric materials and devices have been the center of intense scientific and engineering investigation for many years due to the extraordinary nonlinear optical and electro-optic properties of certain conjugated π-electron systems and due to the fundamental success of molecular engineering in creating new materials with appropriate linear optical, structural and mechanical properties.[1] Organic electro-optic (E-O) materials offer potentially significant advantages over conventional inorganic electro-optic crystals, such as $LiNbO_3$ and GaAs, in several key areas of integrated optics technology, including primary E-O parameters, processing technology and fabrication technology.[2] The most striking advantage, and the reason for the intense interest in these materials, is due to the intrinsic difference in the electro-optic mechanism.[3] Unlike inorganic ferroelectric crystals, where the electro-optic response is dominated by phonon contributions, the electro-optic effect in certain organic materials arises in the electronic structure of the individual molecules, yielding extremely large E-O coefficients with little dispersion from dc to optical frequencies (second harmonic generation) and low dielectric constants.[4] Poled polymer organic materials have been demonstrated which exhibit electro-optic coefficients significantly larger than that of $LiNbO_3$ coupled with a dielectric constant nearly an order of magnitude smaller.[5] The low dielectric constant is essential to the success of high bandwidth modulators due to the resulting lower velocity mismatch between the RF and optical waves, and could lead to an improvement of more than a factor of 10 in the bandwidth-length product over current $LiNbO_3$ devices. The microscopic molecular origin of the second order nonlinear susceptibility, $\chi^{(2)}$, and linear electro-optic coefficient, r, in organic NLO materials is now well understood theoretically and experimentally, and the materials are ready for prototype device implementation.

Equally as important as the primary E-O properties, polymeric integrated optic materials offer far greater fabrication flexibility and processing simplicity than current titanium indiffused $LiNbO_3$ waveguide technology, which requires processing at temperatures approaching 1000°C after expensive and difficult crystal growth. In organic electro-optic materials a nonlinear optical moiety is included in a guest/host or polymer system with appropriate linear optical, mechanical and processing properties, and the desired symmetry is artificially created through electric field poling.[6,7] These materials can then be simply and rapidly spin coated into high quality thin films, processed with standard photolithographic techniques and poled quickly and efficiently. In addition, channel waveguides and integrated optic circuits can be defined by the poling process itself[8], by photochemistry of the E-O polymer[9,10], or by a variety of well understood micro-machining techniques.[11] Furthermore, unlike $LiNbO_3$ where the device structure is limited to one side of a single crystal, multi-layer integrated optic waveguide structures can be fabricated in much the same manner as multilayer multi-chip module substrates. The fabrication flexibility of organic E-O polymers coupled with standard photolithography and fabrication processes makes possible far higher integration densities than are possible with any inorganic integrated optic technology.

In this paper we report our recent progress toward the development of E-O polymer device structures for optical multi-chip modules and related components. These structures include an optical railtap for signal distribution in an integrated optical package, and a high-frequency integrated optic Mach-Zehnder modulator.

2. APPLICATIONS

The recent rapid progress in the development of electro-optic polymer materials and the concomitant success in demonstrating polymer based integrated optic devices has led to wide ranging speculation about applications that can take advantage of the expected superior performance in the primary E-O properties of organic materials. For example, a list of just a few of the applications that we have proposed[12] is given in Table 1. Each of these application areas brings an additional set of requirements on the secondary materials properties, ranging from compatibility with standard process equipment to the stability of the poled state. These "secondary" properties are just as important in determining the ultimate technical and economic practicality of organic electro-optic materials as will the primary properties, such as the electro-optic coefficient and dielectric constant. Before a systems designer will select and use a new technology he must have confidence in the long term stability and reliability of the device prototypes and in the cost effective availability of finished products. The requirements for reliable operation are determined by three factors: 1) the physics of the electro-optic material and device, 2) the manufacturing processes employed to fabricate and package the device, and 3) the end-use and environment in which the finished device must operate. The economic benefit of a new technology over an established one is determined by the cost/performance ratio. Increases in device and system performance must more than make up for any additional costs associated with the new technology. Any deviation from, or addition to, standard manufacturing and assembly equipment and any further restrictions on end-use conditions will significantly increase costs and ultimately limit insertion into systems. As an example, we will briefly discuss optical multi-chip modules in this context.[12]

Table 1. Potential Applications of Electro-Optic Polymer Based Devices.

• OPTICAL MULTICHIP MODULES
• RECONFIGURABLE OPTICAL CONNECTORS
• RECONFIGURABLE OPTICAL BACKPLANES
• HIGH-SPEED MULTIPLEXERS AND DEMULTIPLEXERS
• HIGH-SPEED SWITCHING NETWORKS
• HIGH-SPEED DIGITAL AND ANALOG MODULATOR ARRAYS
• HIGH-SPEED ANALOG-TO-DIGITAL CONVERTORS
• TWO-DIMENSIONAL OPTICAL SOURCE ARRAYS
• PIGTAILED INTEGRATED OPTIC DEVICES
• LINEAR LASERS AND PACKAGES

Great improvements in the operation of semiconductor electronic devices have been made during the last decade. The switching speeds of individual electronic circuits in silicon and GaAs now reach well into the hundreds of megahertz and even the gigahertz regimes. The electrical high density interconnect multi-chip module (MCM) is a new electronic interconnect packaging technology that addresses current generation high speed chips and is just now entering systems implementation. As the package sizes become larger, however, electronic interconnects have difficulty handling the high data rates and interconnection densities required by emerging high speed integrated circuit technology, and optical interconnects become attractive. Optical signals can carry information great distances with minimal loss, crosstalk and excess noise. Consequently, the development of passive optical interconnect technologies that are based on passive polymer waveguides and are compatible with current and projected high speed microelectronics is now underway. In passive optical interconnects, fixed optical waveguides capable of very high speeds and high interconnect densities with minimal crosstalk and attenuation replace the conventional metal interconnections.

The incorporation of active electro-optic polymer switching elements with electronic multichip modules (MCM) and passive optical interconnections may enable optical multi-chip modules (OMCM), as shown schematically in Figure 1. The substrate is overlaid with a multi-layer structure of active and passive organic polymer waveguides, metallic control electrodes, signal paths and insulation layers. In addition to electronic ICs, laser diodes and detector arrays are also mounted on the substrate and electrically connected to the optical devices through very short tabs. Each functional element can be fabricated out of the material with the best performance and using the most efficient process technology, and then efficiently integrated together. A key component of OMCM technology, invented at Lockheed, is an optical rail with active electro-optic taps, which greatly simplifies the process of converting the electrical signals to optical form for distribution throughout

the package. This conversion step is currently one of the greatest impediments to achieving an optical MCM. The design, initial fabrication, and test of an optical railtap is described below. Electro-optic polymer technology may make possible the incorporation of both electronic and optical functionalities in a single highly compact structure, provided the organic materials can meet the thermal and reliability requirements of the electronics industry.

We have conducted a detailed systems analysis comparing an electrical MCM with an optical MCM for a module of area 20 cm^2 in which a microprocessor is connected to 16 Mbytes of SRAM memory.[13] The analysis included design of the output and input buffers on the ICs, the IC technology, the power required to drive the railtap modulators, the power required to drive the laser diodes, the optical power budget in the interconnect network, and the design of the detector and amplifier to regenerate the logic level. SPICE models were run to determine the expected receiver power consumption. For data rates of 50 MHz and above optical interconnects would require significantly less power than electrical interconnects for either CMOS or ECL devices. Above 500 - 1000 MHz electrical interconnects become increasingly more difficult and will not be possible without expensive custom microwave transmission line design. At what frequency, and even whether, optical MCMs become cost competitive with electrical interconnects will be determined by how readily organic electro-optic materials fit into existing electronic fabrication and packaging processes and end-use environments. In the following section we investigate the performance requirements that the electro-optic materials and devices will have to meet in order to be used in MCM applications.

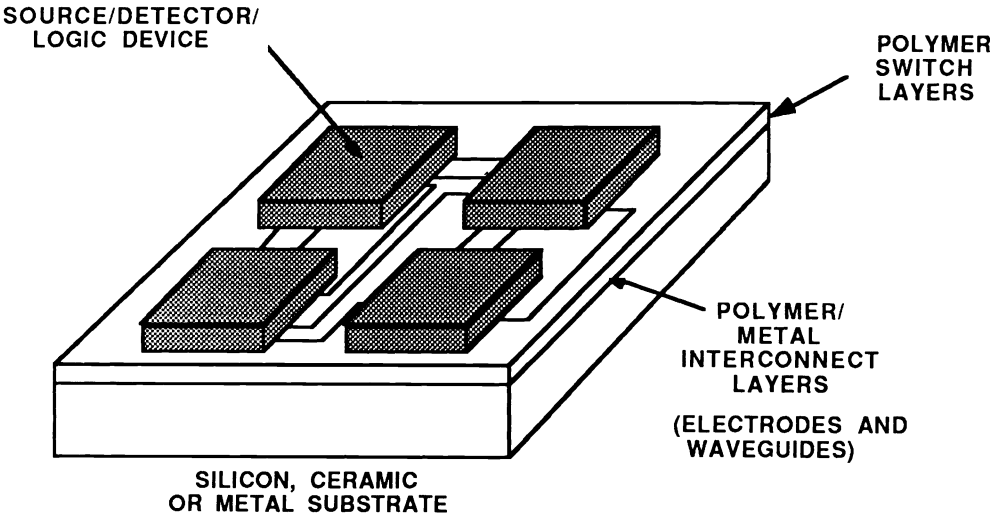

Figure 1. Schematic Diagram of an Optical Multi-Chip Module Based on Electro-Optic Polymers.

3. MATERIALS REQUIREMENTS

The achievement of optical multi-chip modules will require the hybrid assembly of Silicon and/or GaAs integrated circuits, E-O polymer devices, diode lasers, photodetectors, optical fibers, passive polymer dielectrics, metallic power and ground connections and ceramic packages. The E-O polymer devices and optical interconnects must enhance the performance of the electronic system and not impose additional constraints on the fabrication, assembly or use of the electronic assembly. The product performance levels required of such assemblies are already well known through experience with telecommunications optical receiver and transmitter modules and military hybrid microelectronics. Shown in Table 2 is a set of specifications, derived from those established for electronic systems, on the thermal requirements for E-O polymer based modules. The specifications for military applications are given by Mil. Spec. 883c Level 2, and require use to 125°C and storage to 200°C. The generally accepted requirements for commercial applications are only slightly less stringent than those for military applications. Perhaps the most difficult requirements to meet, however, are those imposed by the standard assembly processes used for electronic modules. While the times are relative short, on the order of minutes, the temperatures

reached in packaging and die attach are quite stressing, above 300°C. While these requirements might be reduced somewhat by using nonstandard assembly procedures, this will greatly increase the cost of the product and significantly reduce the likelihood that organic materials can compete on a cost/performance basis.

Table 2. Temperature Requirements for E-O Polymer Integrated Optic Modules.

MIL SPEC 883c LEVEL 2	
USE	- 40 TO 125 ° C
STORAGE	200 ° C
COMMERCIAL	
USE	20 TO 100 ° C
STORAGE	120 ° C
SHORT EXCURSIONS	
FIBER ATTACHMENT	≤ 250 ° C
WIRE BOND	≤ 100 ° C
HERMETIC PACKAGE	≤ 320 ° C
DIE ATTACH	≤ 320 ° C
SUBASSEMBLY	≤ 320 ° C

Films of electro-optic polymers can formed by spin coating, spray coating, or dip coating, but are amorphous as produced and exhibit no second-order electro-optic effects. These materials must then be processed by electric-field poling[8] to achieve a macroscopic alignment in order to enable second-order nonlinear optical effects. In brief, the E-O polymer material is heated above its glass transition temperature, a high electric field is applied by electrodes or a corona to partially align the nonlinear molecules in the direction of the field, and the material is cooled back to room temperature under the influence of the electric field. This process "freezes" in the molecular orientation and creates a macroscopic electro-optic coefficient in the material. The process of electric field poling is both the great advantage of E-O polymers and the great unknown as to their ultimate practicality. The only way to induce electro-optic effects in inorganic materials such as $LiNbO_3$ is to find a naturally non-centrosymmetric crystal and engage in expensive single crystal growth. By comparison, electric field poling is quick and inexpensive and allows molecules with extremely large nonlinearities to be used without regard to the capricious way in which they crystallize. The catch is that the poled state is, of course, not permanently "frozen" in, but is thermodynamically unstable and will decay back to the randomly aligned state with no E-O effect after the passage of enough time. This decay can be very slow and not interfere with the device lifetime, but it is also highly temperature dependent. As the temperature approaches the glass transition temperature the polymer diffusion rates increase greatly and the decay becomes rapid. The current generation of E-O materials with glass transition temperatures of 100 - 150°C are clearly inadequate for electronic systems applications. This fact has been widely recognized, and much effort is now directed toward higher temperature stable E-O polymer materials.[14] The thermal stability can be improved without detriment to the E-O response because the E-O effects arise in the NLO moiety while the thermal properties and alignment dynamics are determined mainly by the backbone or host polymer, provided, of course, that the NLO moiety can itself withstand the thermal cycles.

4. DEVICE RESEARCH

Because the factors affecting the long term thermal stability of the E-O polymer materials are effectively decoupled from the E-O response mechanisms, much can be learned by fabricating and testing prototype integrated optic devices using current generation E-O polymers. In a concurrent engineering approach materials development must be intertwined with device development and, of course, always guided by the systems application and ultimate end-use. In this section we report on the fabrication and initial test of two devices for optical interconnects. The first device, an optical railtap, is a new device invented at Lockheed for the distribution of many optical information channels from a single CW laser diode. An initial proof-of-concept device was fabricated and tested at frequencies up to 100 MHz to demonstrate the optical functionality required for optical interconnection. The second device is a standard architecture integrated optic Mach-Zehnder interferometric

modulator. A sample device with a traveling wave electrode was fabricated and tested at frequencies up to 20 GHz in order to determine the materials performance parameters for E-O polymers and high speed modulation.

4.1 Railtap

A unique solution to the problem of converting the electrical signal to optical form in an optical interconnect is provided through the use of an optical rail and a sequence of railtaps, as shown schematically in Figure 2. The optical railtap is a key enabling component of optical interconnect technology and is made possible by the inclusion of active electro-optic polymers to make the interconnection network itself active.[15] A passive optical waveguide, or rail, routs optical power around the package and acts as an optical power supply. The optical rail runs near the edge of every IC in the package and an optical tap switch is connected to every output pin The purpose of the railtap is to convert the electrical data stream coming off of the IC output pin into a series of bursts of light representing "1"s and "0"s and to place the optical data stream onto an optical channel that routes it to a receiver, which drives an input pin of the receiving IC. The railtap is a compact electro-optic modulator that is fabricated using electro-optic polymer materials and is driven directly by the IC output electrical signal.

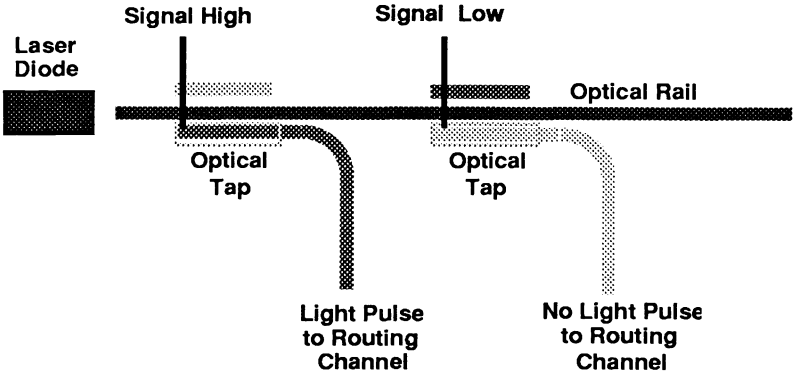

Figure 2. Schematic View of a Railtap for Optical Interconnects.

Several active and passive railtap devices, with up to five taps on a single rail, were fabricated and tested.[16] The dimensions of one such device are shown schematically in Figure 3. This device was diced such that a single tap remained on the central rail and was fabricated in the following manner. First, an aluminium ground plane was deposited on a 3" silicon wafer substrate, and a 4.0 μm thick hard buffer layer was spun coat on top. Next a 2.0 μm layer of the electro-optic material was spun coat. For these experiments an electro-optic polymer material supplied by Akzo Research BV.[9,17] was used. An upper cladding layer of the hard buffer material was then deposited, and a thin 1000Å thick gold poling electrode was deposited. The device was then poled at 130 °C using a poling field of 50 V/μm. After the poling process was completed, the waveguides were formed in the material. The planar gold poling electrode was patterned to form the waveguide definition masking layer using standard photolithographic techniques. The waveguides were then formed by the technique of photobleaching.[9,10] For these experiments, the same gold pattern that defined the waveguides for photobleaching was also used to form the drive electrodes for the initial slow speed device tests. Independent contact was made to each of the electrodes over the channels. The device was inherently slow because the metal electrodes were far larger than necessary and very thin leading to larger resistance and capacitance and thus a lower RC roll-off frequency.

For initial tests on the active railtap, the device was configured for symmetric modulation of light from the center channel to the side taps. With no applied voltage most of the light was coupled out of this channel and only a small amount of leakage was observed. When a voltage is applied, most of the light was switched back into this channel. A modulation depth of approximately 6 dB (optical) was achieved. While this modulation depth represents good performance for these initial test devices, much improved performance is necessary for prototype devices. This device was designed with a short interaction length of only 1 mm for modulation of 1-5% of the light in the central rail, and, in addition, was relatively weakly poled at 50 V/μm. The device was therefore overdriven in order to demonstrate the modulation depth above the leakage background. In an optimized device the off-state leakage would be minimal, and reducing this off-state leakage is crucial to successful systems implementation.

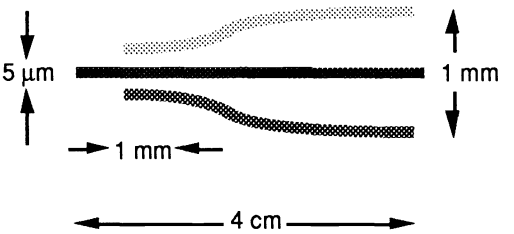

Figure 3. Dimensions of a Sample Single Element Railtap.

The same railtap was driven asymmetrically and modulated in a complementary fashion. Shown in Figure 4 are the intensity line scans of the output endface of the 3 port railtap. In each case the central spot is the optical rail, the signal line is on the right and the complementary signal is on the left. In the righthand picture the signal is applied and a strong beam appears in the signal channel, with almost no light in the complementary channel. In the lefthand picture, the complement of the signal is applied and almost no light appears in the signal channel, while a strong peak appears in the complementary channel. In both cases, the optical power left in the central rail is almost unchanged. This is a critical feature for multiple tap rails, since noise depending on the logic state of the upstream taps will not be imparted to the downstream taps. Approximately 6 dB of modulation depth is observed between the signal and its complement.

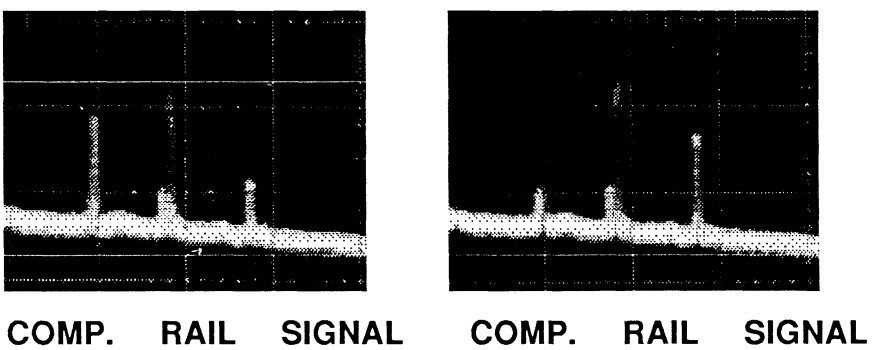

Figure 4. Intensity Line Scan Of the Railtap Endface Showing Complementary Modulation.

The railtap was designed to be only 1mm long for modulation of 1-5% of the light in the central rail and was overdriven to achieve the modulation depth above the leakage background shown in Figure 4. The off-state leakage is due to design, process and fabrication variations leading to deviations from the optimal values of the materials and device parameters, such as waveguide width and index difference. The beam propagation design code was then rerun after fabrication, using the best estimate of the device parameters actually achieved. The results are given in Figure 5, showing a modulation depth close to that actually observed in Figure 4. In addition, this model can be used to estimate the electro-optic coefficient of the polymer. The calculated induced electro-optic coefficient is $r_{33} = 14 \pm 4$ pm/V, in good agreement with that expected from direct measurements on the pure polymer for these poling conditions. This both verifies the predictions of the beam propagation code and indicates that the presence of buffer layers during poling does not greatly alter the induced electro-optic coefficient.

Quantitative measurements of modulation depth and frequency response of the railtap were made by coupling the channel waveguide output to an optical fiber and transmitting it to a photodetector. When a low frequency 20 V voltage swing was applied, a modulation depth of 25% was observed. The frequency response of the railtap was measured with an HP3577A low frequency network analyzer, which has a response from 5 Hz to 200 MHz. Optical fibers were used to endfire couple into and from the channel waveguides and were not permanently attached to the device.

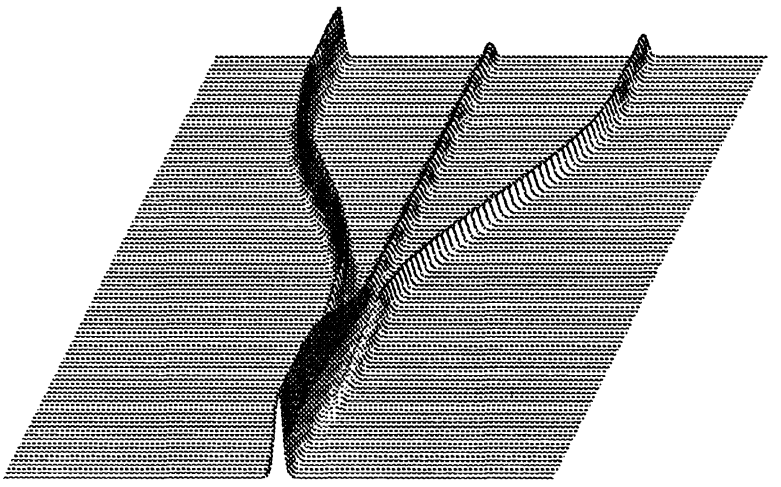

Figure 5. Beam Propagation Model of the Railtap Using Estimate of Actual Device Parameters.

This railtap was not designed for high speed operation. The waveguide masking electrodes were also used as the drive electrodes. These electrodes were made of thin gold approximately 1000Å thick, exhibited relatively high resistance and capacitance, and were not configured as an impedance matched 50 Ω microstrip. The frequency response of this device was expected to be limited by the RC time constant to about 70 MHz. Shown in Figure 6 is the measured frequency response of this railtap. The upper trace is the signal from the railtap when driven with +15 dBm of electrical power for a drive voltage of 3.6 V peak to peak. The railtap response is flat from 50 Hz all the way out to approximately 20 MHz. Although at this point the RC roll-off of the electrode structure begins to reduce the signal, a signal is seen out to 100 MHz. The lower trace is the noise measured with the laser light blocked from entering the device. The vertical axis is a log scale with 10 dB/div (electrical), showing a clear signal more than 30 dB above noise. At higher frequencies rf pick-up is observed.

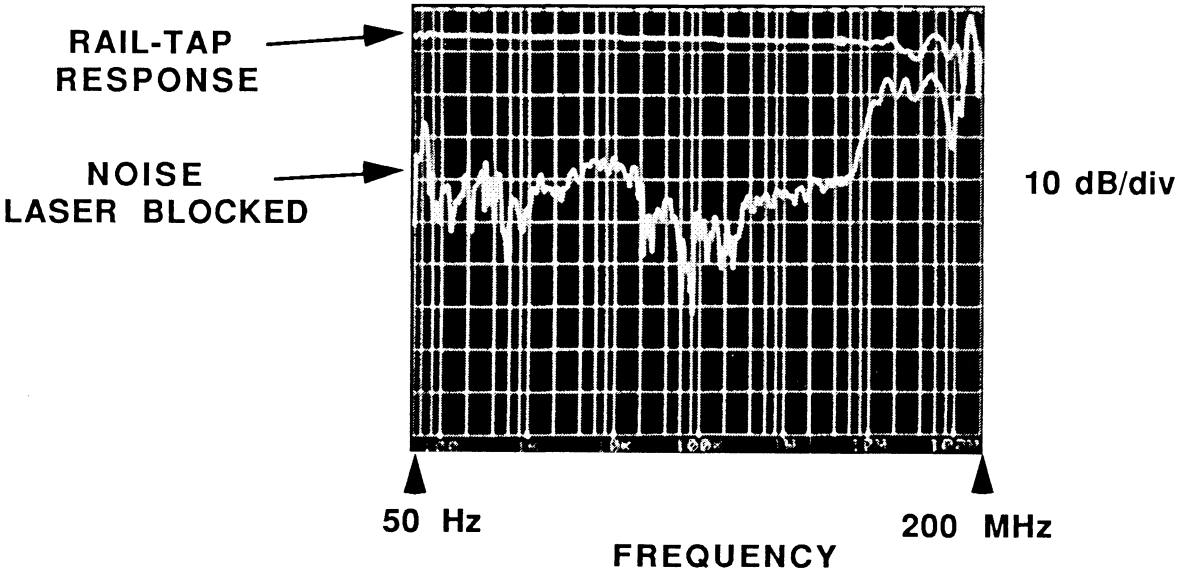

Figure 6. Frequency Response of a "Slow Electrode" Railtap.

4.2 Integrated Optic Mach-Zehnder Interferometer Modulator

A standard Mach-Zehnder integrated optic modulator was fabricated with an impedance matched 50Ω traveling wave electrode in order to investigate the polymeric E-O materials parameters at multi-GHz frequencies.[18] The fabrication process for the high speed modulator was similar to that for the low speed railtaps described above, up through the fabrication of the waveguides. Once again an E-O polymer material supplied by Akzo Research, BV, was used.[9,17]

A schematic diagram of the device, #152, is shown in Figure 7. A 3" silicon wafer with a 1 μm thick aluminium ground plane was used as the substrate, in order to reduce electrode resistance. The three layer buffer/E-O polymer/buffer structure was then spun coat and covered with a thin metal planar photobleaching mask layer. The waveguides were then fabricated by photobleaching exposure under the mask aligner through the waveguide masking layer for three hours. The photobleaching electrodes were removed and the drive electrodes were fabricated.

After the 3" wafer was fabricated, it was diced up and the individual modulators were separated for testing. Four different modulators are made on each 3" wafer, and the final devices are on silicon pieces 1.5" long and 0.5" wide. The modulator was then mounted onto a holder and the center tabs from the input and output electrical SMA connectors are connected to the microstrip electrodes of modulator. Device #152 has waveguides of 5 μm width which are photobleached to a level to ensure single mode operation. The device exhibited a $V_\pi \sim 9$ V and a modulation depth of 10 dB.

Device, #152 had a second microstrip electrode over the second arm of the Mach-Zehnder, as shown in Figure 7. The second electrode was also connected to SMA connectors and allowed independent modulation of each arm. The primary purpose of this change was to enable each arm to be driven independently at a different slightly off-set high frequency. The difference frequency that is generated by mixing these two high frequency phase modulation signals in the nonlinear Mach-Zehnder response makes possible the characterization of the high frequency response of the modulator using intermediate frequency detectors.

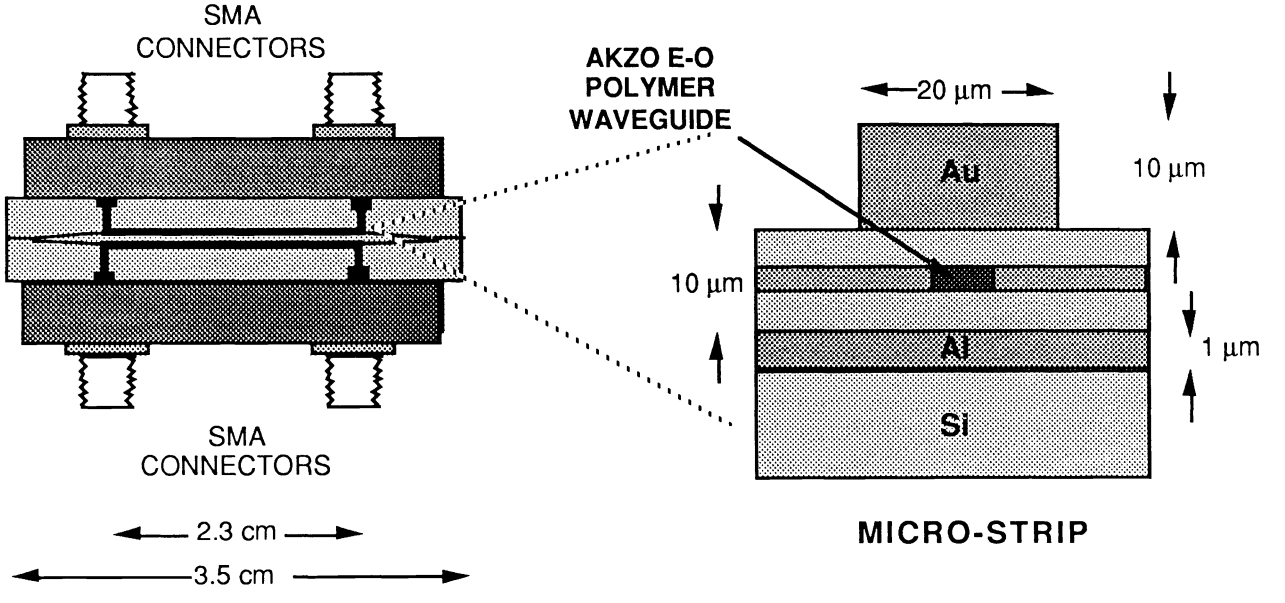

Figure 7. Schematic Diagram of Mach-Zehnder Modulator #152

The optical properties of Mach-Zehnder #152 were first characterized at low frequency. Light from a fiber pigtailed 1.3 μm laser diode was endfire coupled into the device using a selfoc lens assembly. This device is designed to modulate TM polarized light, and a length of polarization preserving single mode fiber was included to allow control of the polarization entering the device. The lens assembly was mounted on a piezoelectrically controlled XYZ stage and two IR vidicons were used to view the input and output endfaces during alignment. After the device was aligned, an output fiber and lens assembly

was used to collect the light from the output of the waveguide structure and transmit it to the detector. A 2 kHz 14 V saw-tooth wave was applied to one device electrode, and the optical output was directed to a detector and observed on an oscilloscope. The optical modulation output exhibited the expected $\cos^2$ dependence and showed clear cusps where the signal turned over. The markers on the oscilloscope were placed at the maximum and minimum points and the voltage necessary to turn the device completely on and off was measured to be $V_\pi = 9V$.

A measurement of the modulation depth of Mach-Zehnder device #152 is shown in Figure 8. Once again a triangle drive voltage is applied and the optical output of the device is measured on a photodetector and an oscilloscope. In this case the light intensity of the on and off states of the modulator is compared to the residual detector noise signal when the laser is turned off and no light is applied. The off-state is ten times lower than the on-state giving a modulation depth of 10 dB. In all of these measurements a large 100 μm core fiber is used to collect the light output of the output waveguide on the device, in order to reduce alignment sensitivity. This is much larger than the 2 μm by 5 μm output waveguide and stray light in the cladding and buffer layers is also collected. It is likely that the actual modulation depth of the device is much better than 10 dB, and we are making efforts improve performance by launching light more efficiently into the input waveguide, reducing scattered light in the cladding and buffer layers and improving the selectivity of the output coupling. The measured half wave voltage of $V_\pi = 9$ V and the modulation depth of 10 dB make possible the evaluation of device # 152 at much higher frequencies, as described below.

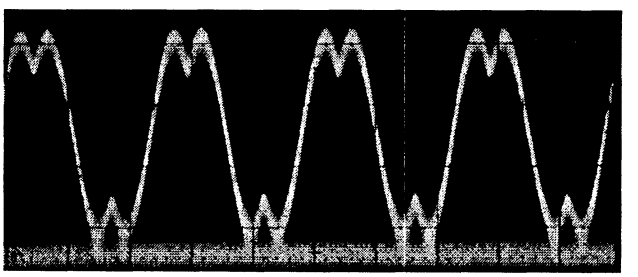

Figure 8. Modulation Depth Measurement of Mach Zehnder 152

The high frequency response of Mach-Zehnder #152 was measured using an HP 8510 network analyzer. Optical fiber pigtails were used to launch 1.3 μm light into the waveguides and to collect the output light and direct it to the detector, in exactly the same manner as for the low frequency measurements described above. For these initial measurements only one electrode over one arm was used and direct detection of the signal was employed. The network analyzer output was used to drive the device microstrip input and the microstrip output was terminated off-chip into 50Ω. The detector electronics consisted of an Optoelectronics PD-50 photodiode with an Avantek AGT 8235 preamplifier and had an aggregate bandwidth of approximately 2 to 8 GHz. Both the detector electronics and the laser were carefully shielded from rf pickup.

The total frequency response of the Mach-Zehnder device #152 plus the response of the detector, the receiver amplifier and the cables connecting the device to the network analyzer from 1 to 11 GHz is shown in Figure 9. A clear modulation response from 20 to 40 dB above the noise floor is observed over the entire receiver bandwidth from 2 to 8 GHz. The signal is strongest at 2 GHz and exhibits a roll-off of approximately 20 dB over the region from 2 to 8 GHz. The signal vanishes above 8 GHz, where the detector is non-responsive. This roll-off is due to the sum of the 6 dB roll-off in the electrode response, the roll-off in the detector, the roll-off in the amplifier and the roll-off in the attenuation of the cables. There is no evidence that there is any roll-off in the response of the electro-optic polymer material.

A series of resonant absorption peaks are also observed in the frequency response shown in Figure 9. These resonances are due to standing waves in the cables and other electrical components that have not been calibrated out of the measurement. The positions of the resonances change when different cables with different lengths are used. Calibration of the electrical portion of the drive and measurement system is now underway.

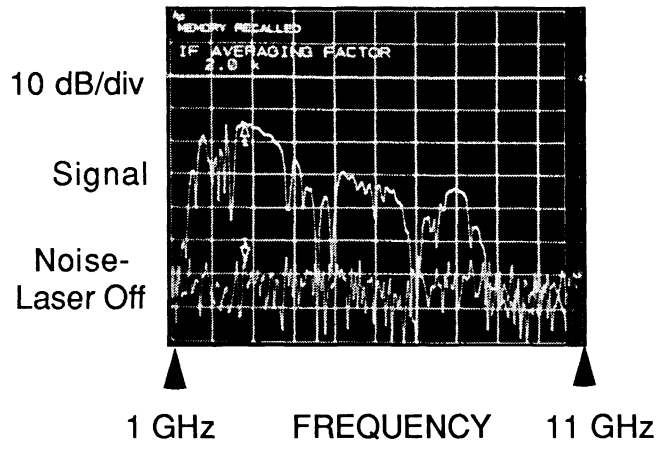

Figure 9. Optical Modulation Response of Mach-Zehnder #152 From 1 to 11 GHz

In order to determine the response of the polymer electro-optic material at frequencies above the current detector bandwidth and to separate roll-off in the detector/amplifier, a heterodyne detection modulation experiment was carried out. A schematic diagram of the experimental set-up is shown in Figure 10. In this case both electrodes over the two arms of the Mach-Zehnder are used. One arm of the Mach-Zehnder was modulated at 20 GHz and the second arm was modulated at 18.5 GHz. In a Mach-Zehnder modulator the optical output intensity is a cosine function of the differential phase delay between the two arms, given by

$$I = I_o[1 + \cos(\phi_1 - \phi_2 + \phi_b)]/2 \qquad (1)$$

where ϕ_1 and ϕ_2 are the phase delays from arms 1 and 2, and ϕ_b is the phase bias resulting from a built-in optical path length difference between the arms or due to an applied DC voltage over one arm. The phase delay in a waveguide under an electrode of length L, with applied voltage V is given by

$$\phi = r_{33} n_o^3 (\pi L/\lambda)(V/d) \qquad (2)$$

where r_{33} is the EO coefficient, n_o is the polymer index of refraction, λ is the wavelength and d is the distance of the electrode to the ground plane.

If sinusoidal voltages are applied to electrodes 1 and 2, with amplitudes V_1 and V_2 at frequencies ω_1 and ω_2, respectively, then

$$\phi_1 = m_1 V_1 \sin(\omega_1 t) \text{ and} \qquad (3)$$

$$\phi_1 = m_2 V_2 \sin(\omega_2 t) \qquad (4)$$

where m_1 is $r33_1 n_o^3(\pi L/\lambda)/d$ and m_2 is $r33_2 n_o^3(\pi L/\lambda)/d$, with $r33_1$ and $r33_2$ being the values of r_{33} at frequencies ω_1 and ω_2, respectively. By substituting (3) and (4) into (1) and expanding into frequency components with Bessel function amplitudes, the output intensity at the difference frequency $(\omega_1 - \omega_2)$ becomes

$$I(\omega_1-\omega_2) = 2I_o(J_1 m_1 V_1)(J_2 m_2 V_2)[\sin(\omega_1 - \omega_2)t][\cos(\phi_b)]. \qquad (5)$$

The existence of a signal at the difference frequency, therefore, provides a heterodyne measurement of the direct modulation at the high frequencies of ω_1 and ω_2 in the two arms of the Mach-Zehnder. The difference frequency at 1.5 GHz was then detected using an Antel APD with a 2.0 GHz bandwidth, as shown in Figure 11. This measurement provides a

proof-of-concept demonstration of electro-optic modulation in a polymer material at 20 GHz. The measurement was limited to 20 GHz only by the available frequency synthesizers and not by any limitation of the device or Akzo E-O polymer.

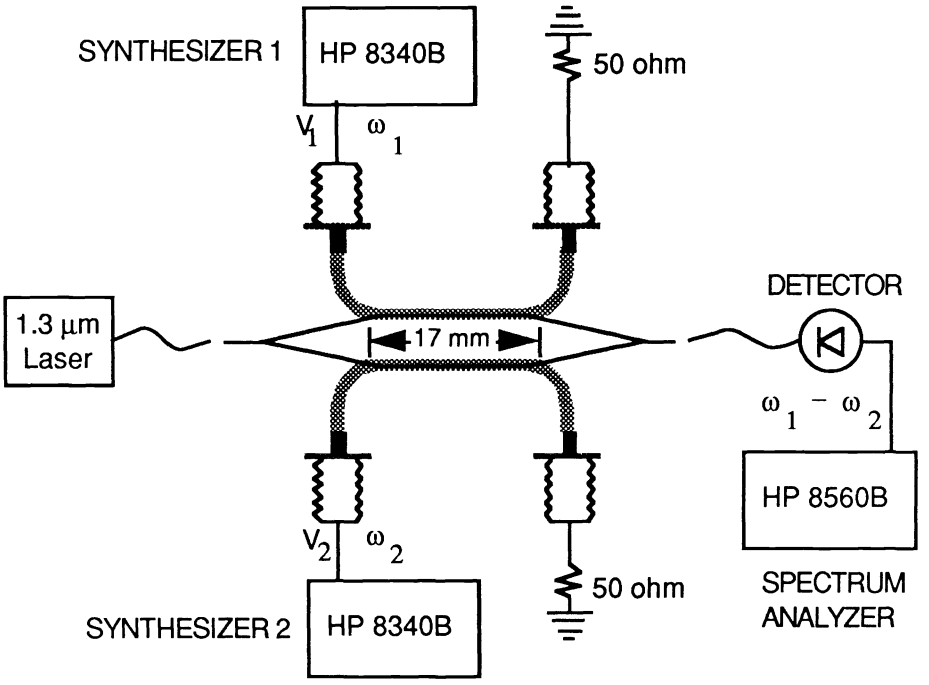

Figure 10. Heterodyne Measurement of the High Frequency Response of Device #152

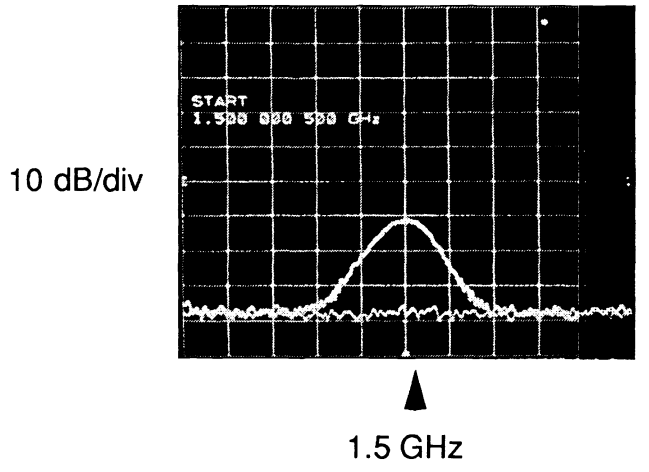

Figure 11. Heterodyne Signal at 1.5 GHz From Drive Signals at 18.5 and 20 GHz

5. SUMMARY AND CONCLUSIONS

We have demonstrated many critical aspects of key components for E-O polymer based optical interconnect systems for electronic applications. An understanding of the E-O polymer materials parameters that will have to be met in an electronic environment has been achieved, and new devices, made possible by the unique properties of E-O polymers, have been

conceived, designed and implemented. Several device demonstrations were carried out using an electro-optic polymer supplied by Akzo Research, BV.[9,17] Passive railtaps were fabricated and tested, and active railtaps with "slow" electrodes were fabricated and operated in both a symmetric and complementary fashion, providing a proof-of-concept demonstration of the modes critical for optical interconnect applications. Modulation depths of 6 dB (optical) were achieved and the frequency response was observed to be flat to 20 MHz and clear modulation was seen at 100 MHz. A standard Mach-Zehnder interferometer modulator with a high speed microstrip electrode was designed, fabricated and tested. This device demonstrated flat material and device response out to 200 MHz on a low frequency testset. The device also showed clear modulation on a high frequency testbed out to 8.0 GHz. A heterodyne measurement technique has been developed and used to measure the E-O response of the modulator to 20 GHz. This is, by far, the highest reported modulation value in any E-O polymer to date.

6. ACKNOWLEDGEMENTS

The research reported in this paper is due to the Lockheed Photonics and Lightwave Technology Group, and is hereby acknowledged with warmth and gratitude. Special acknowledgement is given to Dr. G.R. Mohlmann, Akzo Research, BV, for his participation in the Lockheed research program.

7. REFERENCES

1 Nonlinear Optical Properties of Organic Molecules and Crystals, Vol. 1 and 2, D. Chemla and J. Zyss, ed. (Academic Press, FLA) 1986.

2 R. Lytel, G.F. Lipscomb, and J.I. Thackara, "Recent Developments in Organic Electro-optic Devices", in Nonlinear Optical Properties of Polymers, A.J. Heeger, J. Orenstein, and D.R. Ulrich, ed., Proc. Materials Research Society Vol. 109, 19 (1988).

3 S.J. Lalama and A.F. Garito, "Origin of the Nonlinear Second-order Optical Susceptibilities of Organic Systems", Phys. Rev. A 20, 1179 (1979)

4 K.D. Singer and A.F. Garito, "Measurements of Molecular Second-order Optical Susceptibilities Using DC Induced Second Harmonic Generation", J. Chem. Phys. 75, 3572 (1981).

5 K.D. Singer, J.E. Sohn, and M.G. Kuzyk, "Orientationally Ordered Electro-optic Materials", in Nonlinear Optical and Electro-active Polymers, P.N. Prasad and D.R. Ulrich, ed., Plenum Press, New York (1988), p. 189.

6 K. D. Singer, J.E. Sohn, and S.J. Lalama, Appl. Phys. Lett. 49, 248 (1986), and K.D. Singer, M.G. Kuzyk and J.E. Sohn, "Second-Order nonlinear-optical processors in orientationally ordered materials: relationship between molecular and macroscopic properties", J Opt. Soc. Am. B4, 968 (1987).

7 D.J. Williams, "Nonlinear Optical Properties of Guest-Host Polymer Structures", in Nonlinear Optical Properties of Organic Molecules and Crystals, Vol. 1, D. Chemla and J. Zyss, ed., Academic Press, NY (1987), p. 405.

8 J.I. Thackara, G. G. Lipscomb, M.A. Stiller, A.J. Ticknor and R. Lytel, Applied Physics Letters 52, 1031 (1988)

9 G. R. Mohlmann, W.H. Horsthuis, C.P. van der Vorst, "Recent Developments in Optically Nonlinear Polymers and Related Electro-Optic Devices," Proc. SPIE 1177, 67 (1989)

10 J. Yardley, ACS Spring Meeting, Boston (1990) to be published

11 K. D. Singer, W. R. Holland, M.G. Kuzyk, G. L. Wolk, H.E. Katz, M.L. Schilling, "Second Order Nonlinear Optical Devices in Poled Polymers," Proc. SPIE 1147, 233 (1989)

12 R.S. Lytel, G.F. Lipscomb, J.T. Kenney, E.S. Binkley, and A.J. Ticknor, "Electro-Optic Polymers For Optical Interconnects", Proc. SPIE 1215, 252 (1990).

13 R.S. Lytel, J.T. Kenney, E.S. Binkley and G.F. Lipscomb, to be published.

14 J.W. Wu, J.F. Valley, S. Ermer, E.S. Binkley, J.T. Kenney, G.F. Lipscomb, and R. Lytel, "Thermal Stability of Electro-optic Response in Poled Polyimide Sysyems", submitted to Appl. Phys. Lett.

15 R.S. Lytel , A.J. Ticknor, Patent Pending, and R.S. Lytel, A.J. Ticknor, T.E. Van Eck, G. F. Lipscomb to be published.

16 T.E. Van Eck, A.J. Ticknor, R.S. Lytel and G.F. Lipscomb, to be published.

17 G. R. Mohlmann *et. al.*, Proc. SPIE 1337 (1990).

18 S.L. Kwiatkowski, D.G. Girton, G.F. Lipscomb and R.S. Lytel, to be published.